

# Adaptive strategies for graph state growth in the presence of monitored errors

Earl T. Campbell,\* Joseph Fitzsimons, Simon C. Benjamin, and Pieter Kok  
 Quantum & Nano Technology Group, Department of Materials, Oxford University, Oxford, UK  
 (Dated: June 7, 2018)

Graph states (or cluster states) are the entanglement resource that enables one-way quantum computing. They can be grown by projective measurements on the component qubits. Such measurements typically carry a significant failure probability. Moreover, they may generate imperfect entanglement. Here we describe strategies to adapt growth operations in order to cancel incurred errors. Nascent states that initially deviate from the ideal graph states evolve toward the desired high fidelity resource without impractical overheads. Our analysis extends the diagrammatic language of graph states to include characteristics such as tilted vertices, weighted edges, and partial fusion, which arise from experimental imperfections. The strategies we present are relevant to parity projection schemes such as optical ‘path erasure’ with distributed matter qubits.

PACS numbers: 03.67.Lx, 03.67.Mn, 42.50.Pq

Graph states have the remarkable property that they embody all the entanglement needed for quantum algorithms. The computation then proceeds purely through single-qubit measurements, consuming the graph state as a resource [1, 2, 3]. Several physical mechanisms that can create graph states have been identified, many of which employ measurements in order to create the required entanglement [4, 5, 6, 7, 8, 9, 10]. Efficient graph state creation is possible even when these entangling measurements have a high failure probability, provided that success is heralded [7, 9, 11, 12, 13, 14, 15, 16]. Failure corresponds, at worst, to local (repairable) damage to the growing graph state. This approach has been applied to linear optical scenarios, and to scenarios involving macroscopically separated matter qubits. A successful entangling measurement must have a *high fidelity*: Imperfect (non-maximal) entanglement generally leads to errors in the computation. However, achieving a higher fidelity by enforcing more stringent success criteria will generally result in a large resource overhead [15].

We show that by adaptively altering the growth process of graph states, there is a class of imperfections that can be tolerated in creating ideal graph states. We consider *monitored errors*, i.e. random errors that cannot be predicted but which are known once they have occurred. Such errors may originate from frequency mismatch, spatial mode mismatch, or cavity coupling mismatch. Here, we illustrate our techniques by considering the non-maximal entanglement that occurs when two sources in a path erasure scheme have unequal photon emission rates [17, 18, 19]: A spontaneously emitted photon that is detected early in the detection window is more likely to have originated from the more rapidly emitting cavity; conversely, photon detection late in the window implies a bias to the slower cavity. Rather than abandoning such events as failures, we exploit the fact that the resulting entanglement is a known function of the detection variable (e.g., the observation time). Non-ideal measurements are employed to create ideal graph states, dramatically reducing the resource overhead.

In order to incorporate the effects of monitored errors, we extend the graph state formalism by introducing *tilted vertex amplitudes*, *weighted graph edges* [20, 21], and *partial*

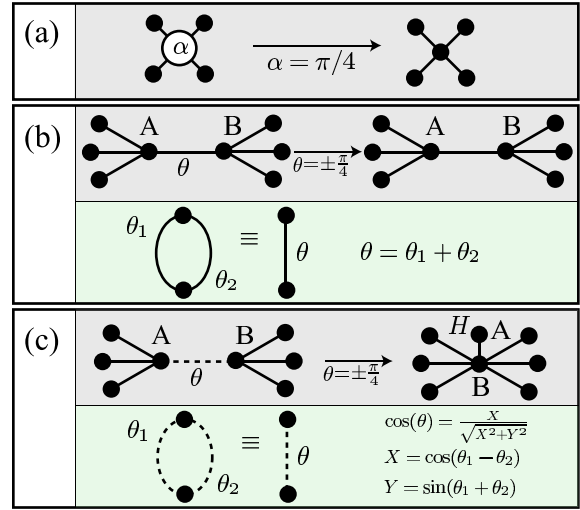


FIG. 1: Graph generalizations (left), the corresponding proper graphs (right), and the relevant addition rules. (a) tilted vertices are hollow circles labelled  $\alpha$ , denoting a qubit in a state  $\cos(\alpha)|0\rangle + \sin(\alpha)|1\rangle$  prior to applying two qubit operations; (b) weighted graph edges, illustrated as a solid edge between two qubits  $A$  and  $B$ , and labelled  $\theta$ . In operator notation a weighted edge is  $U_{AB}(\theta) = \cos(\theta)\mathbb{1} + i\sin(\theta)Z_A Z_B$ ; (c) partial fusions, illustrated as a dashed line between two qubits  $A$  and  $B$  labelled  $\theta$ . In operator notation a partial fusion is  $P_{AB}(\theta) = \cos(\theta)\mathbb{1} + \sin(\theta)Z_A Z_B$ .

*fusions* (see Fig. 1). Tilted vertices arise directly from the monitored errors, whereas weighted edges and partial fusions may result from measurements on tilted vertices. This broader class of multi-qubit states still has a graphical description whose complexity increases only polynomially with the number of qubits. We present three adaptive growth strategies that yield ideal graph states in the presence of monitored errors; we will refer to these as realignment, merging and bridging.

We will consider schemes for graph state construction that use Projective Measurements (PMs) to construct graph states. A PM is a probabilistic entangling operation that, when successful to a high fidelity, results in a projection of two qubits onto the odd parity subspace. An example of such a PM

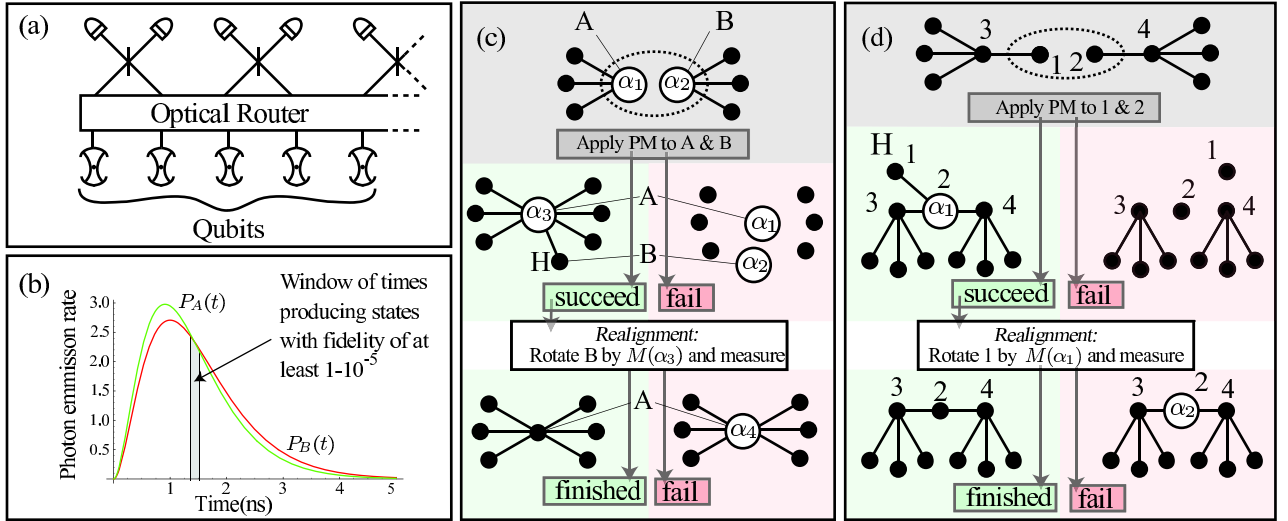


FIG. 2: (a) A distributed quantum computer; the qubits are stored in matter systems which are coupled to optical modes. Pairs of optical paths are routed towards a beam splitter while two detectors (a PM device). (b) emission rates from two mismatched cavities; detection events within the shaded region correspond to high-fidelity entanglement. (c) fusing tilted GHZ states by a projective measurement. Upon success, this will result in a larger tilted GHZ state. This can be probabilistically purified into a proper GHZ state. (d) fusing two cherries generates a tilted central vertex with a single cherry (which is used for realignment). If realignment fails the state can be used for merging (Fig. (3a)) or bridging (Fig. (4a)).

scheme is given in Ref. [4]. In this proposal matter qubits are initially prepared in the state  $|+\rangle \equiv (|0\rangle + |1\rangle)/\sqrt{2}$ . The qubits emit photons depending on their state, and which-path erasure is used to create two-qubit entanglement (Fig. 2a). In the ideal situation, when only a single detector clicks, the qubits are projected onto the maximally entangled  $(|01\rangle + |10\rangle)/\sqrt{2}$  state. However, with partially distinguishable photon sources, the qubits are projected onto a state of the form,  $\cos(\alpha)|01\rangle + \sin(\alpha)|10\rangle$  [22]. If the distinguishability results from the two qubits having different photon emission rates, see Fig. (2b), then knowing the time of the detector click means the value of  $\alpha$  is also known, and hence monitored. With current technology detectors can resolve time several orders of magnitude faster than typical cavity emission times, allowing accurate error monitoring. Thus a dominant error source may be subsumed into our graphical language by the introduction of tilted vertices.

**Tilted vertices** A tilted vertex is parametrised by an angle  $\alpha$ , which defines the initialisation state of that qubit as  $|\psi\rangle = \cos(\alpha)|0\rangle + \sin(\alpha)|1\rangle$ . When the parameter is  $\alpha = \pi/4$  the qubit is a proper vertex, as illustrated in Fig. (1a). Additional graph generalizations will be shown to arise when certain measurements are made on tilted vertices.

**Weighted edges** A weighted graph edge between two vertices  $A$  and  $B$  is defined in operator notation as  $U_{AB}(\theta) = \cos(\theta)\mathbb{1} + i\sin(\theta)Z_A Z_B$ , and is graphically represented as a solid edge labelled with an angle  $\theta$ . The angle is constrained to the range  $-\pi/4 \leq \theta \leq \pi/4$ , by using the identity  $U_{AB}(\theta + \pi/2) = iZ_A Z_B U_{AB}(\theta)$ . A weighted edge  $U_{AB}(\theta)$  is local unitary equivalent to a control- $Z(4\theta)$ ; where  $Z(\varphi)$  is the diagonal matrix with elements  $(1, e^{i\varphi})$ . For brevity these

local equivalences will be omitted, such that weighted edges with  $\theta = \pm\pi/4$  are equivalent to a control- $Z$ , represented by a proper graph edge, as illustrated in Fig. (1b).

**Partial fusions** A partial fusion between two qubits  $A$  and  $B$  is defined in operator notation as  $P_{AB}(\theta) = \cos(\theta)\mathbb{1} + \sin(\theta)Z_A Z_B$ , and is graphically represented by a dashed line labelled  $\theta$ . The angle is again constrained to a  $\pi/2$  range, by the identity  $P_{AB}(\theta + \pi/2) = Z_A Z_B P_{AB}(-\theta)$ . When  $\theta = +\pi/4$  or  $\theta = -\pi/4$ , the operator becomes a projector onto the even or odd parity subspace, respectively, as occurs with type-II fusion [7]. For a full fusion  $P_{AB}(\pm\pi/4)$  on proper vertices, the resulting state is equivalent to a pure graph state, as in Fig. (1c). This last required graph generalization differs from the previous two in its non-unitary nature, and hence there will be an implicit renormalization in all expressions.

We now describe strategies for adapting graph state synthesis in response to monitored errors. The microcluster approach [13] is suitable as the overall scheme: GHZ states are created and selectively fused together in order to produce any desired tologopy. We begin by noting that a simple *realignment* process allows us to correct a tilted vertex through the sacrifice of a neighbour. We then observe that, even without such neighbours, a proper graph can still be constructed using strategies we call *merge* and *bridge*. The steps involved are probabilistic, but upon failure the latter strategies leave residual entanglement which can be exploited in subsequent attempts. The merge procedure is efficient at increasing the size of medium sized GHZ states, while the bridge procedure can create edges between multi-neighbour nodes. Thus these two strategies would be relevant at different stages of the microcluster growth scheme, for example.

**Realignment** The realignment strategy is most clearly described using GHZ states. A proper GHZ state is any proper graph that has no more than one node with multiple neighbours, or any local unitary equivalent graph. The vertex with many neighbours is called the *core* vertex, and the attached single neighbour vertices are its *cherries*. Generalized GHZ states can be constructed by projectively measuring the core qubits of two smaller generalized GHZ states, as illustrated in Fig. (2c). If successful, the state has one tilted vertex to be corrected. The value of  $\alpha_3$  will be determined by  $\alpha_1$ ,  $\alpha_2$ , and the photon detection time; increasing the expected amount of entanglement associated with  $\alpha_3$  is discussed in [22]. A realignment strategy, shown in Fig. (2c), can correct the tilted vertex by measuring a cherry in a basis tuned to  $\alpha_3$ . Note that a tilted vertex could not possibly be corrected through purely local operations on that vertex, since the tilt implies incorrect entanglement relations with the neighbouring vertices. The cherry qubit is rotated by  $M_B(\alpha_3)$ , where  $M(\alpha) = \sin(\alpha)X - \cos(\alpha)Z$ , which becomes  $H$ , the Hadamard, for  $\alpha = -\pi/4$ . With success probability  $p_s(\alpha_3) = \frac{1}{2} \sin^2(2\alpha_3)$  the tilting will be removed. If the realignment is unsuccessful, then the tilting is exacerbated such that its angle changes to  $R(\alpha_3) = \arccos(\cos^2(\alpha_3)(1 - p_s(\alpha_3))^{-\frac{1}{2}})$ . Note that the realignment procedure is not specific to tilted vertices in generalized GHZ states, but can be used to correct any tilted vertex that has a cherry. A less risky procedure, which constructs graph states more complex than GHZ states, requires a PM on two cherries (Fig. 2d). The risk is less because a failure results in only two qubits being separated. When successful one of the qubits becomes a tilted *intercore* vertex, and the other becomes its cherry. Again the cherry can be used for realignment. Through repeated applications of this procedure one could realize any graph topology, including the cubic lattice graphs known as cluster states.

The remainder of this letter concerns what use can be made of this tilted two-neighbour vertex after all of its cherries have been lost. If the tilted vertex is connected to two vertices labelled 3 and 4, then two options are available: (i) to attempt to *merge* 3 and 4 with  $P_{34}(\pm\pi/4)$ , as in Fig. (3); (ii) to attempt to *bridge* 3 and 4 with  $U_{34}(\pm\pi/4)$ , as in Fig. (4).

**Merging** The protocol for the first attempt at merger is shown in Fig. (3a). Note that, if the vertex was not tilted, then this can be deterministically achieved by measuring the intercore vertex in the  $X$ -basis. However, when the vertex is tilted the procedure becomes probabilistic. Either the even  $P_{34}(\pi/4)$  or odd  $P_{34}(-\pi/4)$  parity projector can be targeted by rotating by  $M_2(\alpha_1)$  or  $M_2(-\alpha_1)$ , respectively. Success occurs with probability  $p_s(\alpha_1) = \frac{1}{2} \sin^2(2\alpha_1)$ . Failure creates a partial fusion onto the subspace that is orthogonal to the targeted subspace; hence the sign flipping of  $P_{34}(\mp R(\alpha_1))$ .

The entanglement from this partial fusion will increase the probability of success for subsequent attempts at merging. For another attempt to be made at merging, first a successful PM must be achieved. This will generate a new tilted intercore vertex with a cherry that can be used in a realignment attempt. If realignment is successful, then Fig. (3c) shows how this can

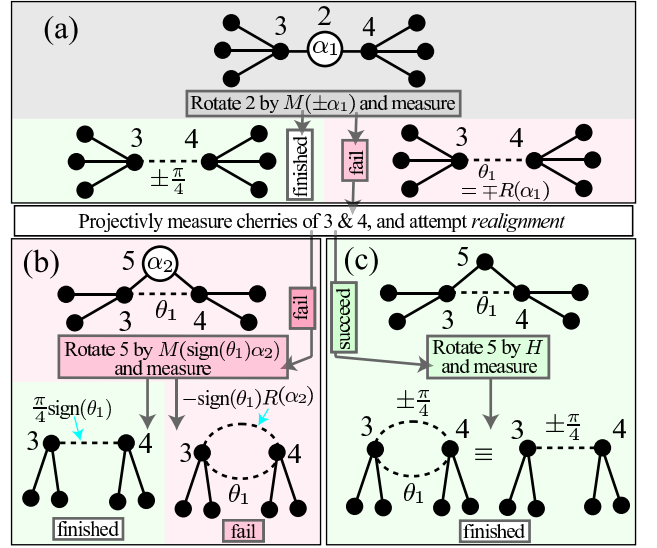


FIG. 3: Connecting two subgraphs by merging one qubit from each subgraph. The qubits are labelled by 3 and 4, and a successful merger corresponds to  $P_{34}(\pm\pi/4)$ . (a) an attempt to merge two qubits attached to a tilted vertex with success outcome  $P_{34}(\pm\pi/4)$  or failure outcome  $P_{34}(\mp R(\alpha_1))$ . After a failure, projective measurements must be repeated until two more cherries are fused. A realignment attempt can then be made on the resulting tilted vertex by measuring its only *cherry*. If realignment is successful then implement (c), but if failed then implement (b). (b) is a probabilistic procedure that on success generates  $P_{34}(\pm\pi)$  and on failure  $P_{34}(\mp R(\alpha_2))$ . (c) is a deterministic procedure that projects with  $P_{34}(\pm\pi/4)$ .

be used to deterministically add to the partial fusion to get a full parity projection, which only differs from the untilted case by skewing the probabilities of the even or odd projection results. If realignment is unsuccessful, then Fig. (3b) shows how a probabilistic attempt can be made at merging. The probability of success is  $p_m(\alpha_2, \theta_1) = p_s(\alpha_2)(1 \pm \sin(2\theta_1))$ , where the sign freedom,  $\pm$ , comes from the chosen rotation  $M(\pm\pi/4)$ . Hence, the partial entanglement will always be beneficial if we match  $\pm$  to the sign of  $\theta_1$ . If this attempt at merging fails then it causes an additional partial fusion of  $P_{34}(-\text{sign}(\theta_1)R(\alpha_1))$ , where the function  $\text{sign}(x)$  equals 1 for positive  $x$ , and  $-1$  otherwise. The two partial fusions can be combined using the rules specified in Fig. (1c).

**Bridging** Having covered the merging procedure, we will now describe the bridging procedure, shown in Fig. (4), which aims to generate  $U_{34}(\pm\pi/4)$ . Fig. (4a) starts with a graph that has a cherryless tilted intercore vertex and no pre-established graph edge between 3 and 4. The rotation  $M_2(\pm\alpha_1) \cdot S$  will target  $U_{34}(\pm\pi/4)$ , where  $S$  is the diagonal matrix with elements  $(1, i)$ . Again the success probability is  $p_s(\alpha_1)$ . A failure results in a weighted edge of an angle  $\mp R(\alpha_1)$ .

In parallel with the merging procedure, Figs. (4c)&(4b) show how to proceed, with another perfect intercore vertex or another tilted intercore vertex, respectively. In contrast with the merging procedure, weighted edges combine by a simple rule of addition. Consequently, the exact amount of

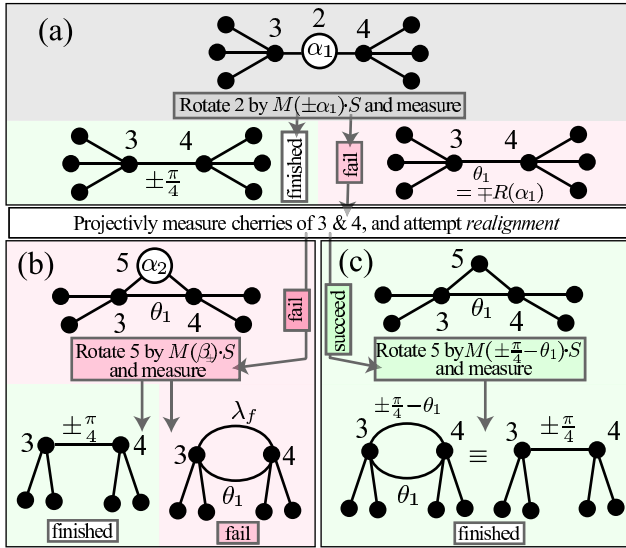


FIG. 4: Connecting two subgraphs by bridging one qubit from each subgraph. The qubits are labeled by 3 and 4, and a successful bridge corresponds to  $U_{34}(\pm\pi/4)$ . (a) an attempt to bridge two qubits attached to a tilted vertex with success outcome  $U_{34}(\pm\pi/4)$  or failure outcome  $U_{34}(\mp R(\alpha_1))$ . After a failure, projective measurements must be repeated until two more cherries are fused. A realignment attempt can then be made on the resulting tilted vertex by measuring its only cherry. If realignment is successful then implement (c), but if it fails then implement (b). (b) is a probabilistic procedure that on success generates  $U_{34}(\pm\pi/4 - \theta_1)$  and on failure  $U_{34}(\lambda_f)$ , where  $\beta_{\pm}$  and  $\lambda_f$  are respectively defined by (1) and (3). (c) is a deterministic procedure that projects with  $U_{34}(\pm\pi/4 - \theta_1)$ .

extra weighted edge must be targeted. Given a pre-existing weighted edge of angle  $\theta_1$  an additional  $U_{34}(\pm\pi/4 - \theta_1)$  is required. However, when the bridging process involves a tilted intercore vertex together with some pre-existing weighted edge (Fig. 4c), calculating the required rotation is more involved. Rotating the tilted vertex by  $M(\beta_{\pm}) \cdot S$  and measuring, causes either  $U_{34}(\pm\pi/4 - \theta_1)$  or  $U_{34}(\lambda_f)$ , when:

$$\beta_{\pm} = N \cos(\alpha_2)(\pm \cos(\theta_1) - \sin(\theta_1)), \quad (1)$$

$$N = (1 \mp \sin(2\theta_1 \cos(2\alpha_2)))^{-\frac{1}{2}}. \quad (2)$$

The targeted  $U_{34}(\lambda_s)$  will be successful with probability  $p_b(\alpha_2, \theta_1) = p_s(\alpha_2)N^2$ . As before, this probability can be made to be always larger than  $p_s(\alpha_2)$ , by using the sign freedom in the rotation  $M(\beta_{\pm}) \cdot S$ . If the measurement fails, then a weighted edge  $U_{34}(\lambda_f)$  is added, where:

$$\cos(\lambda_f) = \arccos \left( \frac{\cos(\theta_1) \cos(\beta_{\pm})}{\sqrt{1 - p_b(\alpha_2, \theta_1)}} \right). \quad (3)$$

*Improvements* A rough measure of the improvement made by our scheme can be reached by calculating the increase in success probability for a single attempt at an entangling operation. Consider two cavities differing in coupling strength by 10% that have the photon emission rates in

Fig. (2b), provided we neglect photon loss. In a naive scheme that post-selects projective measurements with a fidelity of less than  $1 - 10^{-5}$ , the success probability drops from the inherent 50% to only 4%. Our scheme will attempt to bridge or merge any projective measurement that produces a finite amount of entanglement. A successful bridge or merge will, in the limit of ideal detectors, generate unit fidelity entangled states. The overall success probability becomes 24%; a substantial improvement on the naive approach by a factor of 6 [22].

*Conclusions* A realistic model of distributed quantum computing gives rise to an interesting class of random but monitored errors, which are treated as a generalization of graph states. A set of strategies has been presented that adapt the growth scheme to tackle these errors. In some instances a failed attempt generates a state that is described by further graph generalizations, but these states possess partial entanglement that is recycled in later attempts. The benefit of the scheme is that high-fidelity graph states can be constructed when using cavities with varying physical parameters without suffering the severe loss in success probability that comes with a naive post-selection strategy.

*Acknowledgements* We would like to thank Dan Browne and Peter Rohde for useful comments on the manuscript. This research is part of the QIP IRC (GR/S82176/01). SCB acknowledges support from the Royal Society.

\* Electronic address: earl.campbell@materials.ox.ac.uk

- [1] R. Raussendorf and H. J. Briegel, Phys. Rev. Lett. **86**, 5188 (2001).
- [2] R. Raussendorf et al., Phys. Rev. A **68**, 022312 (2003).
- [3] M. Hein et al., Phys. Rev. A **69**, 062311 (2004).
- [4] S. D. Barrett and P. Kok, Phys. Rev. A **71**, 060310(R) (2005).
- [5] Y. L. Lim et al., Phys. Rev. Lett **95**, 030505 (2005).
- [6] Y. L. Lim et al., Phys. Rev. A **73**, 012304 (2006).
- [7] D. E. Browne and T. Rudolph, Phys. Rev. Lett **95**, 010501 (2005).
- [8] S. C. Benjamin et al., New J. Phys. **7**, 194 (2005).
- [9] S. C. Benjamin et al., New J. Phys **8** (2006).
- [10] D. E. Browne et al., Phys. Rev. Lett **91**, 067901 (2003).
- [11] E. Knill et al., Nature **409**, 46 (2001).
- [12] N. Yoran and B. Reznik, Phys. Rev. Lett. **91**, 037903 (2003).
- [13] M. A. Nielsen, Phys. Rev. Lett. **93**, 040503 (2004).
- [14] P. Kok et al., (2006), quant-ph/0512071.
- [15] L. M. Duan and R. Raussendorf, Phys. Rev. Lett **95**, 080503 (2005).
- [16] D. Gross et al., (2006), quant-ph/0605014.
- [17] S. Bose et al., Phys. Rev. Lett **83**, 5158 (1999).
- [18] X. L. Feng et al., Phys. Rev. Lett **90**, 217902 (2003).
- [19] C. Cabrillo et al., Phys. Rev. A **59**, 1025 (1999).
- [20] W. Dür et al., Phys. Rev. Lett. **94**, 097203 (2005).
- [21] S. Anders et al., (2006), quant-ph/0004051.
- [22] E. T. Campbell et al., (In Preparation).